New Nonsymmetric $P(OH)_3$ Species. Comparison with the C_3 Isomer and Themochemistry at the DFT, MP2, and CCSD(T) Levels of Theory

L. Maron[†] and A. Ramírez-Solís*[,‡,§]

Laboratoire de Physique Quantique, IRSAMC, Université Paul Sabatier, 118, Route de Narbonne Toulouse 31062 Cedex, France, and Department of Chemistry & Biochemistry, University of California at Santa Barbara, Santa Barbara, California 93106-9510

Received: January 2, 2007; In Final Form: February 27, 2007

Two new less-symmetric $P(OH)_3$ isomers that are more stable than the C_3 structure are found at the density functional theory (B3PW91, B3LYP), MP2, and CCSD(T) levels with the large aug-cc-pvdz/pvtz basis sets. The C_1 and C_3 structures are qualitatively different from those found for the $As(OH)_3$ molecule. An additional lower lying $P(OH)_3$ structure with C_s symmetry has been obtained. With the largest basis set the C_s isomer is predicted to be the most stable. However, the inclusion of zero-point-energy corrections induces an inversion between the C_s and C_1 isomers, with the latter becoming the lowest energy structure at the highest correlated level. Increasing inclusion of electronic correlation effects reduces the energy difference between the C_1 and C_s structures while the C_1-C_3 energy difference and C_1-C_s interconversion barrier become larger. In all cases, energy differences and barrier heights are around 1 kcal/mol.

I. Introduction

In a recent study we have shown[1] the existence of a nonsymmetric C_1 $As(OH)_3$ species in the gas phase that is slightly more stable than the previously known C_3 one. We reported there the new bare optimized structure and its associated energy barrier to the symmetric C_3 structure, obtained through HF, DFT (B3LYP), MP2, MP4, and CCSD(T) calculations using increasingly large Gaussian basis sets. We showed that the quantum zero-point-energy (ZPE) vibrational effects are essential to provide accurate thermochemical values. The infrared spectra were calculated at the MP2/aug-cc-pVTZ (AVTZ) level to characterize the global C_1 and local C_3 minima, as well as the transition state.

$As(OH)_3$ is thought to be the main species that is biologically active and responsible for many of the toxic and carcinogenic reactions caused by arsenic-polluted water.[2−4] Although the structural features of $As(OH)_3$ in solution are relevant to characterize the species that gets imported into cells, we have stressed that no implications of the existence of this new C_1 isomer are envisaged in relation to the As−O coordination environment in solution, mainly because the interaction energies with the solvating environment are much larger than the minute energy differences found between these two isomers and, also, due to the larger conformational changes of $As(OH)_3$ induced by solvation than those involved in the C_1-C_3 interconversion.[1,5]

Since nitrogen, phosphorus, antimony, and bismuth belong to the same group as arsenic in the periodic table, it is reasonable to expect that $N(OH)_3$, $P(OH)_3$, $Sb(OH)_3$, and $Bi(OH)_3$ also have C_1 isomers that are slightly more stable than the corresponding C_3 known structures. As a first step in the elucidation of this hypothesis, we have very recently studied the $N(OH)_3$ case, both statically[6] using the same quantum chemical methodology that allowed us to firmly characterize the greater stability of the C_1 structure of $As(OH)_3$, and dynamically through atom-centered basis Born−Oppenheimer ab initio molecular dynamics (AIMD)[7] simulations at room temperature. These AIMD studies led to the discovery of a new even more stable C_s isomer of $N(OH)_3$.[8]

In this article we shall focus on the second member of the $X(OH)_3$ (X = N, P, As, Sb, Bi) family. We study the structural stability of several isomers of the $P(OH)_3$ molecule, which plays very important roles in many biochemical systems,[9] using the same accurate quantum chemical methodology that allowed us to firmly characterize the greater stability of the C_1 and C_s structures for $As(OH)_3$ and $N(OH)_3$.

II. Method: Quantum Chemical Calculations

Ab initio MP2, MP4(SDQ), CCSD(T), and density functional theory (DFT) based calculations were done for the (closed-shell singlet) C_3 and for the new C_1 $P(OH)_3$ structures; the latter was derived from the recently found C_1 isomer of $N(OH)_3$.[6] We stress that two possible C_3 structures exist: one equivalent to the $As(OH)_3$ C_3 "cuplike" form (see Figure 1a of ref 1) and another, "spiderlike" structure where the OH bonds point "upward", in the opposite direction of the P−O bonds (see Figure 1c of ref 6), equivalent to the stable C_3 form of $N(OH)_3$. All geometry optimizations are fully unconstrained and used the large optimized augmented correlation-consistent polarized valence double-ζ and triple-ζ (aug-cc-pVDZ or AVDZ, aug-cc-pVTZ or AVTZ) basis sets of Dunning.[10] For the DFT calculations two hybrid but different (B3PW91 and B3LYP) exchange-correlation functionals were used as programmed in the Gaussian 98 code.[11] The transition states (TS) linking either the C_1 and C_s geometries or the C_s and C_3 geometries were found using the reactants-to-products quasi-synchronous transit (QST2) algorithm as programmed in Gaussian 98; the TS were further characterized by vibrational analysis showing a single imaginary frequency at the DFT (with both functionals) and MP2 levels with both basis sets. The connection between the

* Corresponding author. E-mail: alex@servm.fc.uaem.mx.
† Université Paul Sabatier.
‡ University of California at Santa Barbara.
§ On sabbatical leave from Depto. de Física, Facultad de Ciencias, Universidad Autónoma del Estado de Morelos, Av. Universidad 1001, Cuernavaca, Morelos. 62209 México.

10.1021/jp070020o CCC: $37.00
Published on Web 03/30/2007

TABLE 1: B3LYP/AVDZ and MP2/AVDZ Optimized Geometries; Main Parameters for the MP2 Optimized Structures with AVTZ Basis Sets[a,b]

	MP2/AVTZ				
$P(OH)_3$	C_1	$TS_{C_1 \rightarrow C_s}$	C_3	$TS_{C_s \rightarrow C_3}$	C_s
distances					
P−O1	1.665	1.653	1.640	1.653	1.647
P−O2	1.637	1.645	1.640	1.650	1.637
P−O3	1.635	1.642	1.640	1.654	1.647
O1−H1	0.964	0.964	0.965	0.967	0.964
O2−H2	0.968	0.969	0.965	0.967	0.969
O3−H3	0.968	0.965	0.965	0.967	0.964
bond angles					
O1−P−O2	93.9	99.9	97.3	99.8	101.8
O2−P−O3	101.5	96.7	97.3	99.5	91.7
O3−P−O1	103.1	100.5	97.3	100.4	101.8
P−O1−H1	111.4	110.2	110.6	110.8	110.2
P−O2−H2	111.7	111.2	110.6	111.1	111.8
P−O3−H3	111.5	111.7	110.6	111.2	110.2
dihedral angles					
O1−P−O2−H2	−166.5	−114.6	−97.8	−99.7	−92.5
O1−P−O3−H3	89.3	143.4	163.7	2.7	165.1
O2−P−O1−H1	−10.9	−23.9	163.4	10.3	−47.1
O2−P−O3−H3	91.8	74.8	−98.2	−91.3	47.1
O3−P−O1−H1	49.2	113.5	−97.8	−97.6	−165.1
O3−P−O2−H2	−47.7	12.1	163.8	4.3	92.5

[a] Distances are in angstroms and angles in degrees. [b] The optimized geometries are available upon request in *Z*-matrix format.

obtained TS and the related minima has been verified using an intrinsic reaction coordinate (IRC) calculation available in Gaussian 98.

For the highest correlated ab initio method used here, CCSD(T), single-point calculations were done using the MP2 optimized geometries for the largest basis set; the zero-point-energy (ZPE) contributions were obtained using the MP2/AVTZ harmonic vibrational frequencies and these were applied to correct the CCSD(T) electronic energies, as previously done for the $As(OH)_3$[1] and $N(OH)_3$[6,8] cases.

III. Results and Discussion

A. Optimization and Starting Geometries. As mentioned in the previous section, in order to obtain the stable C_3 isomer it seemed natural to start with either the equivalent "cuplike" structure of the $As(OH)_3$ molecule or the "spiderlike" structure of the $N(OH)_3$ molecule. As in the previously reported results on $N(OH)_3$,[6] the "cuplike" geometry of $P(OH)_3$ was found to be an unstable C_3 structure showing two imaginary frequencies, whereas the "spiderlike" C_3 structure led to true minima at all levels of theory. Moreover, a C_s structure similar to the one found by AIMD simulations for $N(OH)_3$[8] has been found on the potential energy surface (PES) of $P(OH)_3$. This means, of course, that the passage from the C_3 structure to the either a C_1 or a C_s one has to proceed through TS of similar geometries compared with those obtained for the $N(OH)_3$ molecule. The C_1 and C_s structures were found in the $N(OH)_3$ molecule to be the lowest in energy, and only the interconversion between the C_3 and C_s structures had been studied.[8] The conversion between the C_1 and C_s isomers for $P(OH)_3$ has now also been investigated.

B. Geometries and Vibrational Spectra. Table 1 shows the P−O distances, O−P−O angles, and O−P−O−O dihedral angles for the optimized geometries of the new C_1 and C_s, the C_3 species, and the corresponding $TS_{C_1 \rightarrow C_s}$ and $TS_{C_s \rightarrow C_3}$ at the MP2 level using the largest (AVTZ) basis sets. It has been shown for $As(OH)_3$[1] and $N(OH)_3$[6] that the optimized geometries were actually not very dependent on the level of theory used.

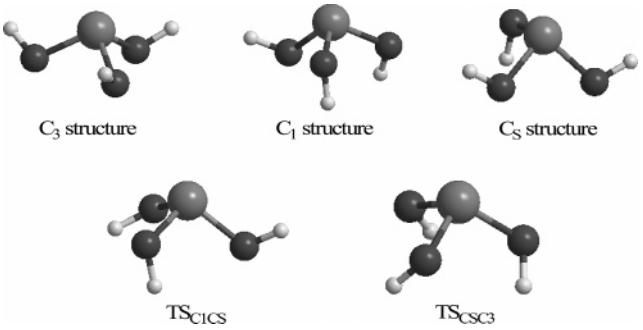

Figure 1. MP2/AVTZ optimized structures for all stationary points in the PES.

The optimized MP2/AVTZ structures for all optimized stationary points in the $P(OH)_3$ PES are depicted in Figure 1. It should be noted that, for the C_1 isomer, the P−O distances show three slightly different P−O bonds at 1.665, 1.637, and 1.635 Å, with two shorter P−O bonds. Note that, at this level of theory, the optimized C_1 isomer is very close to a C_s structure. However, we stress that the true C_s isomer has two longer P−O bonds at 1.647 Å and a single short bond at 1.637 Å. Given the very small energy differences between the C_1 and C_s isomers, we point out that basis set quality becomes a crucial issue; this is shown by the inversion in relative stability found when going from the AVTZ to the AVTZ basis at the MP2 level. Note that at the CCSD(T)/AVTZ level the energies of the C_1 and C_s isomers are very close to each other, only 0.03 kcal/mol apart, and the C_s isomer remains the lowest lying structure.

Since we are dealing with the same transition states as in previous studies on $N(OH)_3$ and $As(OH)_3$, the corresponding transition states for $P(OH)_3$ turned out to be also very unsymmetrical (see Figure 1), as in the $N(OH)_3$ case.[6] We recall that for the $As(OH)_3$ molecule the interconversion TS between the C_1 and C_3 structures is much closer to the C_3 symmetric stable isomer,[1] and following Hammond's principle, this fact has energetic implications that are verified quantitatively in Table 2 of that reference.

A quite large 250 cm^{-1} MP2/AVTZ imaginary frequency was obtained at the TS geometry associated with the interconversion mode between the C_1 and C_s structures; for comparison, the C_1-C_3 interconversion frequency for the $As(OH)_3$ molecule is 3 times smaller.[1] On the other hand, this value is close to the one found for the C_1-C_3 interconversion in $N(OH)_3$.[6] A similar result is obtained for the transition structure linking the C_s and C_3 structures; the associated MP2/AVTZ imaginary frequency is found to be 154 cm^{-1} for this transition state.

In Figure 2 we show the MP2/AVTZ infrared spectra (with Lorentzian convolution) for the C_1 (a), the C_s (b), and the C_3 (c) isomers, respectively, which can perhaps be used as reference data to compare with experimental IR results obtained in the gas phase in the near future. At this point we note that, although not readily visible at the scale shown in Figure 2, the expected number of degenerate frequencies for each symmetry type (with axis of order 1, 2, and 3 for the C_1, C_s, and C_3 cases, respectively) isomer is in agreement with the computed IR spectra; the IR MP2/AVTZ frequencies are available upon request for all isomers and for the corresponding interconversion TS.

C. C_1-C_s Energy Difference: Influence of the Correlation Effects, Basis Set, and ZPE. As mentioned earlier, an ab initio quantum molecular dynamics study on $N(OH)_3$ has shown that a C_s stable structure exists and, moreover, that this structure was the global minimum at the B3PW91/6-31G** level of

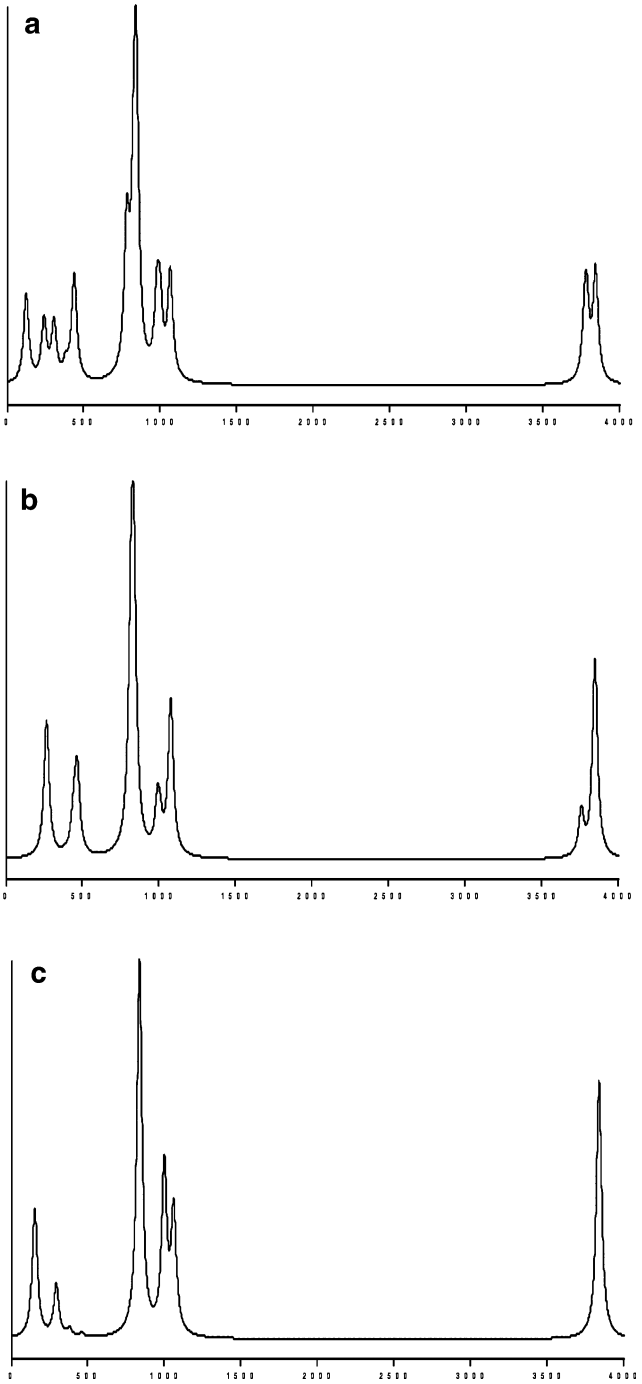

Figure 2. IR spectra calculated at the MP2/AVTZ level (a) for the C_1 species, (b) for the C_s species, and (c) for the C_3 structure. Frequencies in wavenumbers; intensities in arbitrary units. IR tables are available from the authors upon request.

theory. The greater stability of the C_s isomer was later confirmed at the MP2/AVTZ and CCSD(T)/AVTZ levels.[8] This C_s stable structure was also found for $P(OH)_3$, and the energy difference with the C_1 structure has been computed (see Table 2) with different levels of electronic correlation. As can be seen, the increase of the electronic correlation from DFT (B3PW91) to MP2 has very little effect on the energy difference for a given basis set. It should be noticed that the B3LYP results are somewhat different from the other two, even though the energy range is very narrow (a few tenths of a kilocalorie per mole).

The effect of the basis set quality is much more important. Indeed, using an AVDZ basis, the C_1 structure is predicted to be more stable than the C_s one. It should be noticed that the two structures are very close in energy and are almost degenerate, but still a slightly more stable C_1 structure is obtained. Increasing the size of the basis set to AVTZ leads to an inversion of the global minimum. The C_s structure is then predicted to be more stable than the C_1 at the DFT (B3PW91), MP2, and CCSD(T) levels with the considerably larger AVTZ basis set. The B3LYP results are, again, qualitatively different, and the C_1 structure is still predicted to be slightly more stable than the C_s one (but almost degenerate). The increase of the size of the basis set, and therefore its quality, had a larger stabilizing effect on the C_s structure than on the C_1 structure.

TABLE 2: Energy Differences at Different Levels of Theory Using the AVDZ and AVTZ Basis Sets with and without ZPE Corrections in kcal/mol[a]

$P(OH)_3$ structure	B3PW91	B3LYP	MP2	CCSD(T)[b]
transition state $C_1 \rightarrow C_s$				
AVDZ	1.78	1.82	1.85	
with ZPE	1.58	1.54	1.61	
AVTZ	1.73	1.75	1.79	1.81
with ZPE	1.48	1.50	1.49	1.51
C_s				
AVDZ	0.07	0.20	0.07	
With ZPE	0.38	0.46	0.29	
AVTZ	−0.15	0.01	−0.18	−0.03
with ZPE	0.14	0.29	−0.02	0.13
transition state $C_s \rightarrow C_3$				
AVDZ	2.36	2.42	2.78	
with ZPE	1.99	2.04	2.32	
AVTZ	2.81	2.54	2.83	2.64
with ZPE	1.93	1.67	1.93	1.74[c]
C_3				
AVDZ	2.31	2.51	2.63	
with ZPE	2.45	2.55	2.64	
AVTZ	1.82	2.06	1.97	2.13
with ZPE	1.96	2.21	1.74	1.90

[a] Energies are given with respect to the C_1 isomer except for both TSs, whose energies are given with respect to the lowest of the two minima that are connected by each TS structure. [b] Single-point calculations using the MP2 optimized geometries; ZPE corrections from the MP2 vibrational frequencies used for the CCSD(T) corrected energies. [c] Note the disappearance of the interconversion barrier with the inclusion of the ZPE correction.

Given the rather small energy differences, the inclusion of ZPE effects is mandatory and again changes the situation. The inclusion of the ZPE increases the energy difference between the C_1 and C_s structures, favoring the former. However, we note that the ZPE effects for MP2 are about half those obtained with DFT-based descriptions. Thus, using the AVDZ basis set, the C_1 structure is predicted by all methods to be the global minimum, whereas using the AVTZ basis set the C_s structure is still found to be the minimum at the MP2 level but no longer at the DFT (B3PW91) and at CCSD(T) levels. Note that, after inclusion of the ZPE effects, the B3PW91 and CCSD(T) results are in good agreement. This good agreement between the highly correlated ab initio method with the much cheaper semiempirical hybrid exchange-correlation functional was already observed for $N(OH)_3$.[6]

Overall, the PES appears to be rather flat around the C_1 and C_s minima so that changes in electronic correlation treatment, basis set quality, or inclusion of ZPE effects qualitatively change the relative stability of these isomers. However, it should be kept in mind that the ZPE has been calculated using the harmonic approximation (and at the MP2 level for each basis set), which has been shown to possibly lead to inaccurate results when extremely flat PES are investigated. A solution to overcome this problem was proposed by Raynaud et al.[7] in the framework of ab initio molecular dynamics to properly include

the thermal effects. Therefore, this harmonic ZPE vs nonharmonic approximation issue is currently being studied using ab initio molecular dynamics simulations and will be the subject of a future report[12] on $P(OH)_3$.

D. Energy Barrier for the C_1-C_s Conversion: Role of ZPE Effects. As can be seen from Table 2, the energy barrier varies depending on the correlation method in a range of 0.1 kcal/mol, using either the AVDZ or AVTZ basis sets. In that context, and as already shown in the previous section, the inclusion of ZPE effects plays a crucial role. This was also found to be the case for $N(OH)_3$ and $As(OH)_3$. As expected, the inclusion of ZPE effects decreases the energy barrier between the C_1 and C_s structures. This is in agreement with the fact that the inclusion of the ZPE changes the nature of the global minimum. The two structures are found to be very close in energy, and the interconversion is expected to proceed via a low-lying transition state, which involves the change of one short-to-long P−O bond.

The situation is similar to that found for $As(OH)_3$, but different from the $N(OH)_3$ case. Increasing the basis set size, the energy barrier slightly decreases. The inclusion of ZPE effects also decreases the barrier, at all levels of theory. We point out here that, unlike the dramatic ZPE effects found at the MP2, MP4(SDQ), and CCSD(T) levels for $As(OH)_3$, where the ZPE-corrected barriers disappeared with both basis sets,[1] for $P(OH)_3$ the C_1-C_s barriers are found to remain around 1.5−1.8 kcal/mol, showing smaller changes.

E. C_3 Isomer. Before the ZPE effects are considered, note that increasing the quality of electronic correlation treatment (i.e., −hybrid xc functional − MP2 − CCSD(T) order), the C_1-C_3 energy difference becomes significantly larger using the AVTZ basis set. However, when the B3LYP functional is applied, this difference increases to the value already obtained at the CCSD(T) level. The situation is almost the same as the one observed for the C_1-C_s difference.

The effect of the basis set is also found to be important. Indeed, the increase of the basis set size leads to a decreasing of the C_1-C_3 energy difference, as mentioned before for the C_1-C_s case. Thus, the increase of the basis set size favors the most symmetric structure.

The ZPE effects increase the relative stability of the C_3 isomer as compared with the C_1 one, at all levels of theory using the AVDZ basis set. On the other hand, using the AVTZ basis set, the ZPE effects increase the C_1-C_3 energy difference at the DFT level, but lead to a smaller difference at the MP2 and CCSD(T) levels. We note that the decrease at the CCSD(T)/AVTZ level might be somewhat biased, since the ZPE correction was taken from the MP2/AVTZ calculation. Thus, a full geometry optimization at the CCSD(T) level, not affordable so far with the large basis sets used here for the C_1 isomer, would have perhaps led to a slightly different result.

The energy barrier between the C_s and C_3 structures becomes smaller with increasingly accurate electronic correlation effects. This is in agreement with a greater stabilization of the C_3 isomer with respect to the C_s. On the other hand, the increase of the basis set size was shown to preferentially stabilize the C_s structure (becoming the global minimum), leading to an increase of the energy barrier. As expected, the inclusion of the ZPE effects decreases the energy barrier, at all levels of theory.

It is clear that such small energy differences make the experimental observation of two structurally distinct isomers a very difficult task and a refined cryogenic experimental vibrational study in the gas phase is required. The inclusion of ZPE effects is essential given the minute energy differences involved. Note that since our "best" ZPE-uncorrected energy barrier is only 1.15 kcal/mol at the CCSD(T)/AVTZ level, even thermal fluctuations at temperatures as low as 600 K allow very rapid interconversion processes through vibrational excitation between these isomers. Also, it should be noted that, at all levels of theory used here, the flatness of the potential energy surface around the critical points (the C_1, C_s, and C_3 minima and the transition states) poses problems for a truly accurate description, since nonnegligible contributions from the anharmonic terms may actually lead to vibronic couplings that link the "separate" wells of the C_1 and the more symmetric C_s and C_3 structures. Further work is thus needed to obtain a deeper understanding of the role of these higher order vibrational contributions to the corresponding enthalpies. A detailed ab initio quantum molecular dynamics[13] study has been started to address this issue in greater depth.

IV. Conclusions

We have characterized as three minima the C_1, C_s, and C_3 (local) isomers of $P(OH)_3$ and determined the geometry of the transition states linking these structures through very accurate quantum chemical calculations, including electronic correlation effects up to the CCSD(T) level with the large augmented correlation-consistent polarized valence double- and triple-ζ basis sets of Dunning. In all cases the single-reference wave function was found to be adequate for later correlated descriptions. The geometry of the C_3 species is qualitatively different from that found for the $As(OH)_3$ molecule. Both the barriers and the C_1-C_3 energy differences are in the 1.5−2 kcal/mol range, almost twice as large as those found for the $As(OH)_3$ case.

The zero-point-energy corrections are found to play essential roles, and their importance has been assessed through the use of different basis sets and increasing sophistication in the electronic correlation treatments. At the CCSD(T) level, the MP2 optimized geometries and vibrational spectra were used to include the ZPE corrections; although this leads to barrier collapse at the CCSD(T) level with the largest basis set, the C_s isomer remains more stable than the C_1 one.

Within the DFT framework, it was found that the B3PW91 and B3LYP exchange-correlation functionals lead to a different behavior of the energy barriers when increasing the basis set quality, with only the former being in agreement with the highly correlated CCSD(T) method. Therefore, we conclude that the results obtained from DFT calculations on these $X(OH)_3$ species, particularly the energetic ones, should carefully be analyzed and critically compared with high-quality ab initio results when large basis sets are used.

The very small enthalpy difference and energy barriers for interconversion between the C_s, the C_3, and the new C_1 structures undoubtedly make the experimental detection of these distinct species a very difficult task. Using our best ZPE-corrected ab initio value (CCSD(T)/AVTZ), we estimate that the C_1 to C_3 interconversion barrier can be surmounted at temperatures roughly above 600 K. However, even below that threshold the small purely enthalpic difference between the C_1 and C_3 species will lead to almost equivalent populations of both isomers in the gas phase at very low dilution (neglecting the entropic contribution from eventual clustering/aggregation processes). We provide theoretical infrared spectra for these species in the hope that some experimental evidence of the existence of the nonsymmetric species can be found in low-temperature gas-phase experiments in the near future.

Finally, it is clear that the existence of the less-symmetric structures for $As(OH)_3$, $N(OH)_3$, and $P(OH)_3$ allows the pos-

sibility that similar less-symmetric structures could exist also for the isovalent $Sb(OH)_3$ and $Bi(OH)_3$ molecules; work is under way to study the relative stability of these species.[12]

Acknowledgment. A.R.-S. acknowledges support from CONACYT Project 45986-E and FOMES2000-SEP through theproject "Cómputo científico" for unlimited CPU time on the IBM-p690 supercomputer at UAEM, and the UCMEXUS/CONACYT program for sabbatical support at UCSB.

References and Notes

(1) Ramírez-Solís, A.; Hernández-Cobos J.; Vargas, C. *J. Phys. Chem. A* **2006**, *110*, 7637.

(2) Smith, A. H.; Hopenhayn-Rich, C.; Bates, M. N.; Goeden, H. M.; Hertz-Picciotto, I.; Duggan, H. M.; Wood, R.; Kosnett, M. J. Smith, M. T. *Environ. Health Perspect.* **1992**, *97*, 259.

(3) Rosen, B. P. *FEBS Lett.* **2002**, *529*, 86.

(4) Liu, Z.; Shen, J.; Carbrey, J. M.; Mukhopadhyay, R.; Agre, P.; Rosen, B. P. *Proc. Natl. Acad. Sci. U.S.A.* **2002**, *99*, 6053.

(5) Ramírez-Solís, A.; Mukopadhyay, R.; Rosen, B. P. Stemmler, T. *Inorg. Chem.* **2004**, *43*, 2954.

(6) Maron, L.; Ramírez-Solís, A. *J. Mol. Struct. (THEOCHEM)* **2006**, *802*, 111.

(7) Raynaud, C.; Maron, L.; Daudey, J. P.; Jolibois, F. *Phys. Chem. Chem. Phys.* **2004**, *6*, 4226.

(8) Jolibois, F.; Maron, L.; Ramírez-Solís, A. *Chem. Phys. Lett.* **2007**, *435*, 34.

(9) See, for instance: Saint-Martín, H.; Vicent, L. E.; Ramírez-Solís, A.; Ortega-Blake, I. *J. Am. Chem. Soc.* **1996**, *118*, 12167, and references therein.

(10) Dunning, T. H., Jr. *J. Chem. Phys.* **1989**, *90*, 1007. Kendall, R. A.; Dunning, T. H., Jr.; Harrison, R. J. *J. Chem. Phys.* **1992**, *96*, 6796.

(11) Frisch, M. J.; Trucks, G. W.; Schlegel, H. B.; Scuseria, G. E.; Robb, M. A.; Cheeseman, J. R.; Zakrzewski, V. G.; Montgomery, J. A., Jr.; Stratmann, R. E.; Burant, J. C.; Dapprich, S.; Millam, J. M.; Daniels, A. D.; Kudin, K. N.; Strain, M. C.; Farkas, O.; Tomasi, J.; Barone, V.; Cossi, M.; Cammi, R.; Mennucci, B.; Pomelli, C.; Adamo, C.; Clifford, S.; Ochterski, J.; Petersson, G. A.; Ayala, P. Y.; Cui, Q.; Morokuma, K.; Rega, N.; Salvador, P.; Dannenberg, J. J.; Malick, D. K.; Rabuck, A. D.; Raghavachari, K.; Foresman, J. B.; Cioslowski, J.; Ortiz, J. V.; Baboul, A. G.; Stefanov, B. B.; Liu, G.; Liashenko, A.; Piskorz, P.; Komaromi, I.; Gomperts, R.; Martin, R. L.; Fox, D. J.; Keith, T.; Al-Laham, M. A.; Peng, C. Y.; Nanayakkara, A.; Challacombe, M.; Gill, P. M. W.; Johnson, B.; Chen, W.; Wong, M. W.; Andrés, J. L.; González, C.; Head-Gordon, M.; Replogle, E. S.; Pople, J. A. *Gaussian 98*, version A.11.3; Gaussian, Inc.: Pittsburgh, 2002.

(12) Maron, L.; Jolibois, F.; Ramírez-Solís, A. Work in progress.

(13) Maron, L.; Ramírez-Solís, A. Unpublished data.